Electronic Supplementary Material (ESI) for Journal of Materials Chemistry A.
This journal is © The Royal Society of Chemistry 2017

Electronic Supplementary Material

Composite Hollow Nanostructures Composed of Carbon-coated Ti^{3+} Self-doped TiO_2-Reduced Graphene Oxide as an Efficient Electrocatalyst for Oxygen Reduction

Ramireddy Boppella,[a] Ji-Eun Lee,[a] Filipe Marques Mota,[a] Jin Young Kim,[b] Zhenxing Feng,[c] and Dong Ha Kim[a,d,*]

[a]Department of Chemistry and Nano Science, Division of Molecular and Life Sciences, College of Natural Sciences, Ewha Womans University, 52, Ewhayeodae-gil, Seodaemun-gu, Seoul 03760, Korea.

[b]Fuel Cell Research Center, Korea Institute of Science and Technology, 5, Hwarang-ro 14-Gil, Seongbuk-Gu, Seoul 02792, Korea

[c]School of Chemical, Biological, and Environmental Engineering, Oregon State University, 1500 SW Jefferson St., Corvallis, OR 97331, USA

[d]Division of Chemical Engineering and Materials Science, College of Engineering, Ewha Womans University, 52, Ewhayeodae-gil, Seodaemun-gu, Seoul 03760, Korea

* Correspondence: dhkim@ewha.ac.kr

Experimental Section

Synthesis of PS microspheres

Monodispersed polyvinylpyrrolidone (PVP)-modified polystyrene (PS) microspheres were synthesized by dispersion polymerization method using styrene as monomer, 2,2'-azobisisobutyronitrile (AIBN) as an initiator, and PVP as stabilizer. Ideally PVP (4 g) was dissolved in ethanol (55 ml) and purged under Ar flow for 30 min, before adding the styrene monomer (6.4 ml) and AIBN (1 wt%) pre-dissolved in ethanol (5 ml). After polymerization at 70°C for 24 h, monodispersed PS microspheres with an average 1μm diameter were obtained. The formed PS microspheres were consecutively washed with ethanol and centrifuged thrice, before being re-dispersed in ethanol (15 wt.% solution).

Synthesis of graphene oxide (GO)

GO was synthesized by the modified Hummers method [1]. In brief, graphite powder (1 g) was added to 70 ml H_2SO_4 (98%). $KMnO_4$ (3 g) and $NaNO_3$ (0.5 g) were then added gradually in an ice bath. The mixture was stirred for 4 h, after which deionized water (100 ml) was added to the mixture. The resulting preparation was maintained at that temperature for 30 min. A H_2O_2 solution (30%) was then gradually added into the solution while stirring until the suspension turned to brilliant brown indicating fully oxidization of graphite. The mixture was washed repeatedly with 5% HCl, DI-water and collected by centrifugation. The obtained graphite oxide powder was added to ethanol and exfoliated by sonication for 6 h. The resulting suspension was centrifuged for 30 min at 3000 rpm to remove precipitates and used to obtain a stable GO-ethanol suspension. The GO-ethanol suspension was further centrifuged at high rpm to separate exfoliated GO nanosheets.

Characterization techniques

The surface morphology was characterized using scanning electron microscopy (SEM; JEOL JSM6700-F) and transmission electron microscopy (TEM; JEOL JSM-2100F operated at 200kV). Synchrotron XRD were obtained by synchrotron X-ray diffraction (SXRD) at beamline 17-BM at Advanced Photon Source (APS) at Argonne National Laboratory (ANL). Samples were attached to Kapton® tapes and measured in transmission mode. A PerkinElmer® amorphous silicon flat panel detector was used to collect two-dimensional XRD data. Integration of the 2D data to conventional plots of intensity versus 2-theta was performed with Program GSAS(II) [2]. The wavelength used was 0.72768 Å. Raman spectra were recorded on a T64000 (HORIABA Jobin Yvon, France). X-ray photoelectron spectroscopy (XPS) spectra were measured on a Thermo Scientific K-Alpha XPS, using a dual beam source and ultra-low energy electron beam for charge compensation. X-ray absorption near edge spectroscopy (XANES) was carried out in transmission mode at beamline 9-BM of APS, ANL. Data reduction and data analysis were performed with the Athena software packages. The pre-edge was linearly fitted and subtracted. The post-edge background was determined by using a cubic-spline-fit procedure and then subtracted. Normalization was performed by comparing the data to the height of the absorption edge at 50 eV. The monochromator was detuned to 80% of the maximum intensity at those Ti K edges to minimize the presence of higher harmonics. The X-ray beam was calibrated using the Ti metal foil K edge at 4966 eV.

Calibration of SCE and conversion to RHE

The calibration of SCE reference electrode is performed by modified method describe in literature[3]. A standard three-electrode system was utilized with Pt/C deposited glassy carbon electrode and polished Pt wires as the working and counter electrodes respectively, and the SCE as the reference electrode. Electrolytes are pre-purged and saturated with high purity H_2. Linear scanning voltammetry (LSV) is then run at a scan rate of 0.1 mV s^{-1}, and the potential at which the current crossed zero is taken to be the thermodynamic potential (vs. SCE) for the hydrogen electrode reactions. The zero current point observe at -0.998 V, so $E_{(RHE)}=E_{(SCE)}+0.998$ V.

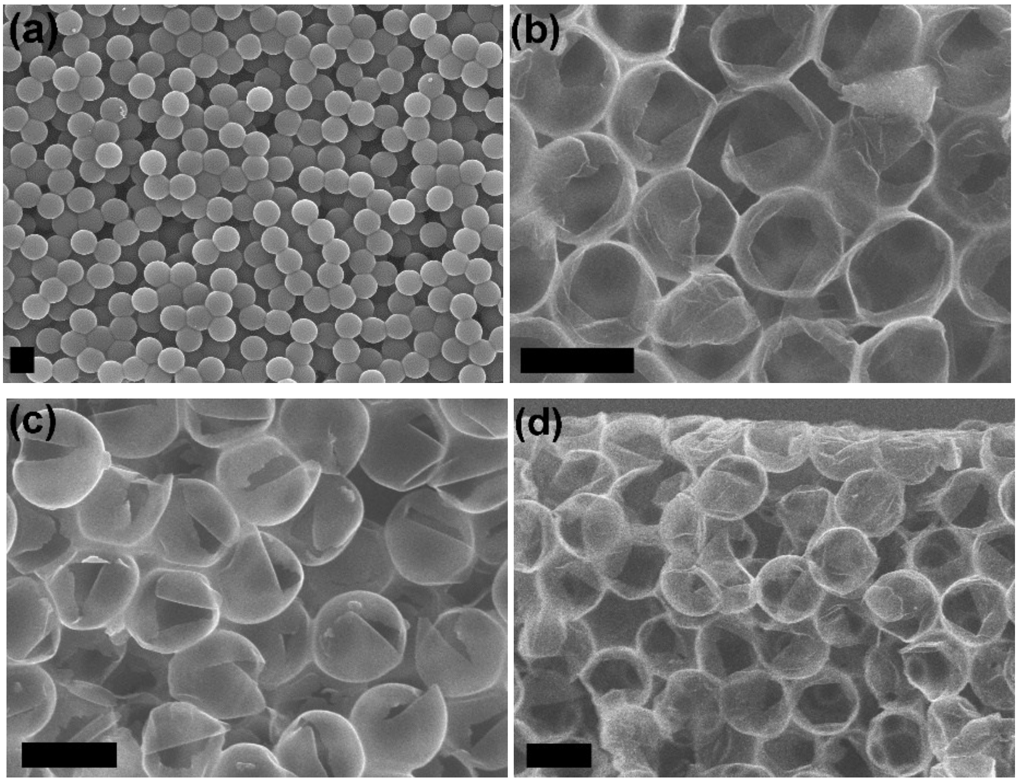

Fig. S1 Low resolution FESEM images of different hollow spheres; (a) PS@TiO_2, (b) rGO(5%)/TiO_2 hollow spheres, (c) rGO(20%)/TiO_2 hollow spheres and (d) cross sectional image of rGO(10%)/TiO_2 hollow spheres. Scale bar is 1μm in all figures

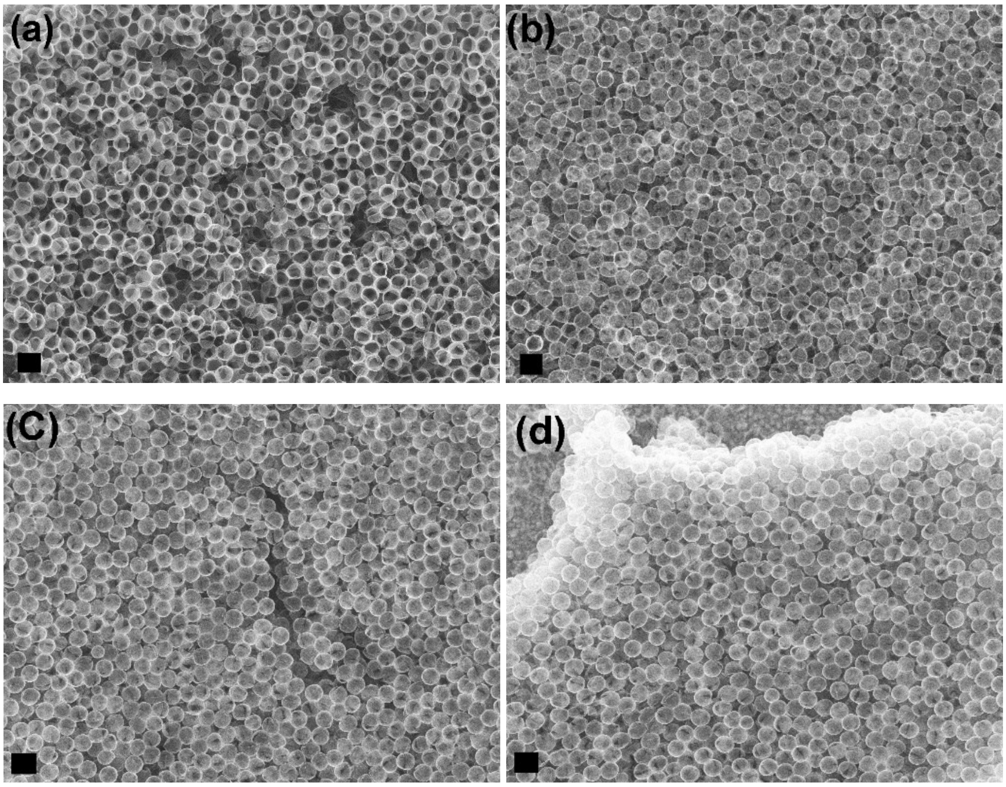

Fig. S2. Low resolution SEM images of hollow spheres. (a) TiO_2 (air), (b)TiO_2, (c) rGO(5%)/TiO_2 and (d) rGO(10%)/TiO_2. Scale bar is 1 μm in all figures

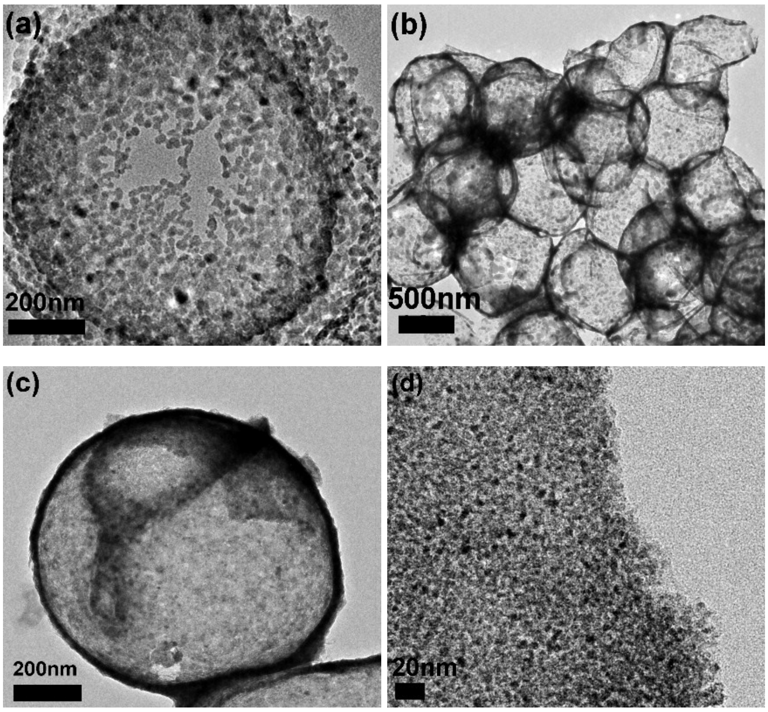

Fig. S3 TEM images (a) TiO_2(air), (b) TiO2, (c) rGO(20%)/TiO_2 showing the hollow nature and (d) HRTEM image of rGO(20%)/TiO_2

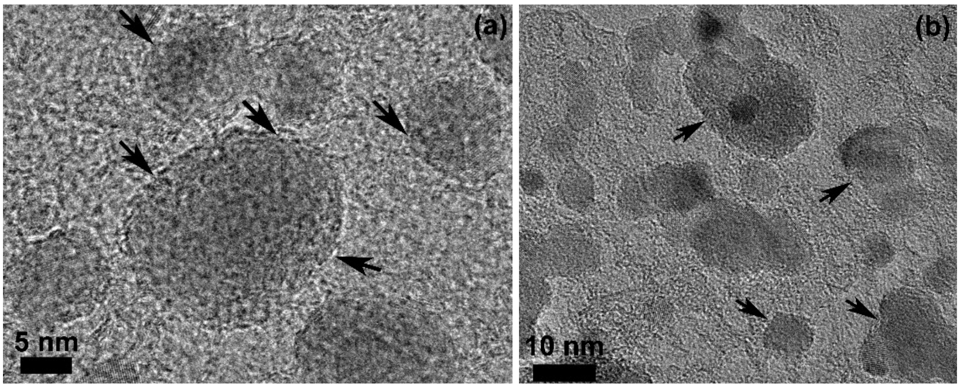

Fig. S4 HRTEM images (a) rGO(5%)/TiO_2 and (b)) rGO(20%)/TiO_2 showing the carbon coated TiO_2 nanoparticles anchored on the rGO sheets

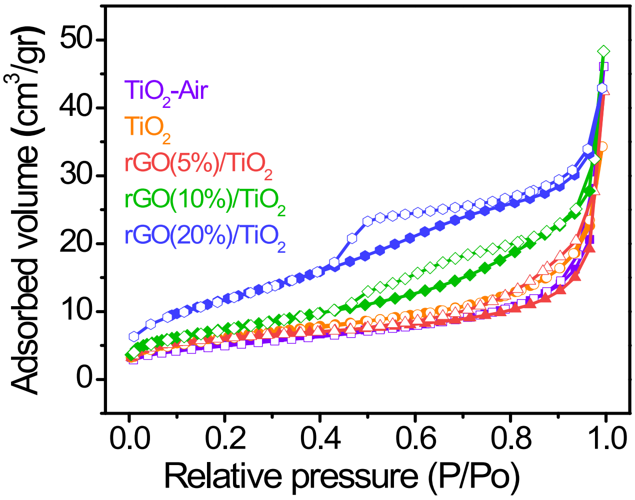

Fig. S5 Nitrogen adsorption-desorption isotherm of different samples

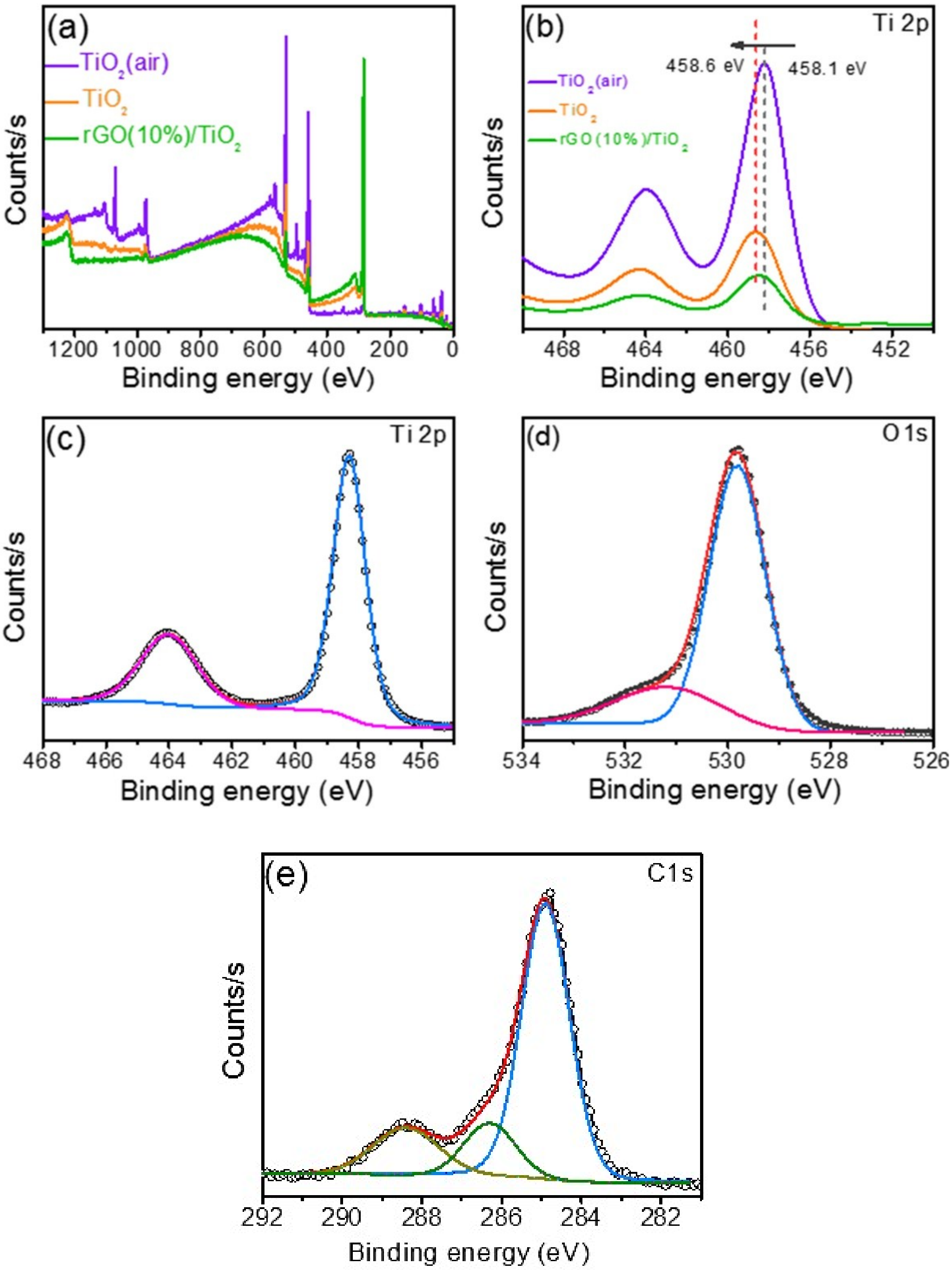

Fig. S6 XPS spectra of TiO$_2$(air), TiO$_2$ and rGO(10%)/TiO$_2$ hollow spheres indicating different chemical composition. (a) the totla survey scan spectrum TiO$_2$(air), TiO$_2$ and rGO(10%)/TiO$_2$ hollow spheres, (b) high resolution Ti2p core level of TiO$_2$(air), TiO$_2$ and rGO(10%)/TiO$_2$ hollow spheres (c) high resolution Ti2p core level of TiO$_2$(air) hollow spheres, (d) O1s spectra of TiO$_2$(air) and (e) C1s core level specra of TiO$_2$(air) hollow spheres.

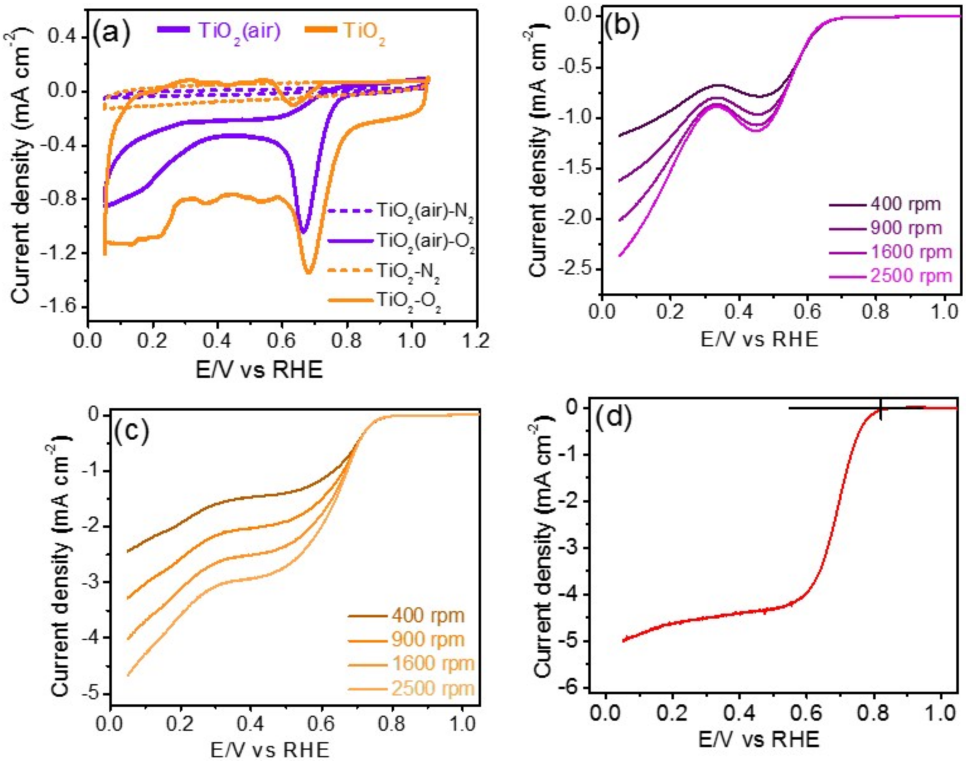

Fig. S7 (a) CV curves of TiO_2(air) and TiO_2 on glassy carbon electrodes in O_2-saturated (solid line) or N_2-saturated 0.1M KOH (dash line), (b) and (c) are LSV curves of TiO_2(air) and TiO_2 respectively, in O_2-saturated 0.1M KOH with a sweep rate of 5mVs^{-1} at the different rotation rates indicated, and (d) schematic representation to determine the onset potential in the present study.

Table S1. Electrochemical parameters of different sample

Sample Name	Current density at 0.1 V @ 1600 rpm	Onset potential	Half wave potential
TiO_2(air)	2.0 mA cm^{-2}	0.70 V	0.54 V
TiO_2	4.0 mA cm^{-2}	0.75 V	0.64 V
rGO(5%)/TiO_2	4.5 mA cm^{-2}	0.78 V	0.68 V
rGO(10%)/TiO_2	5.0 mA cm^{-2}	0.82 V	0.70 V
rGO(20%)/TiO_2	5.5 mA cm^{-2}	0.82 V	0.70 V
Pt/C	5.4 mA cm^{-2}	1.01 V	0.82 V

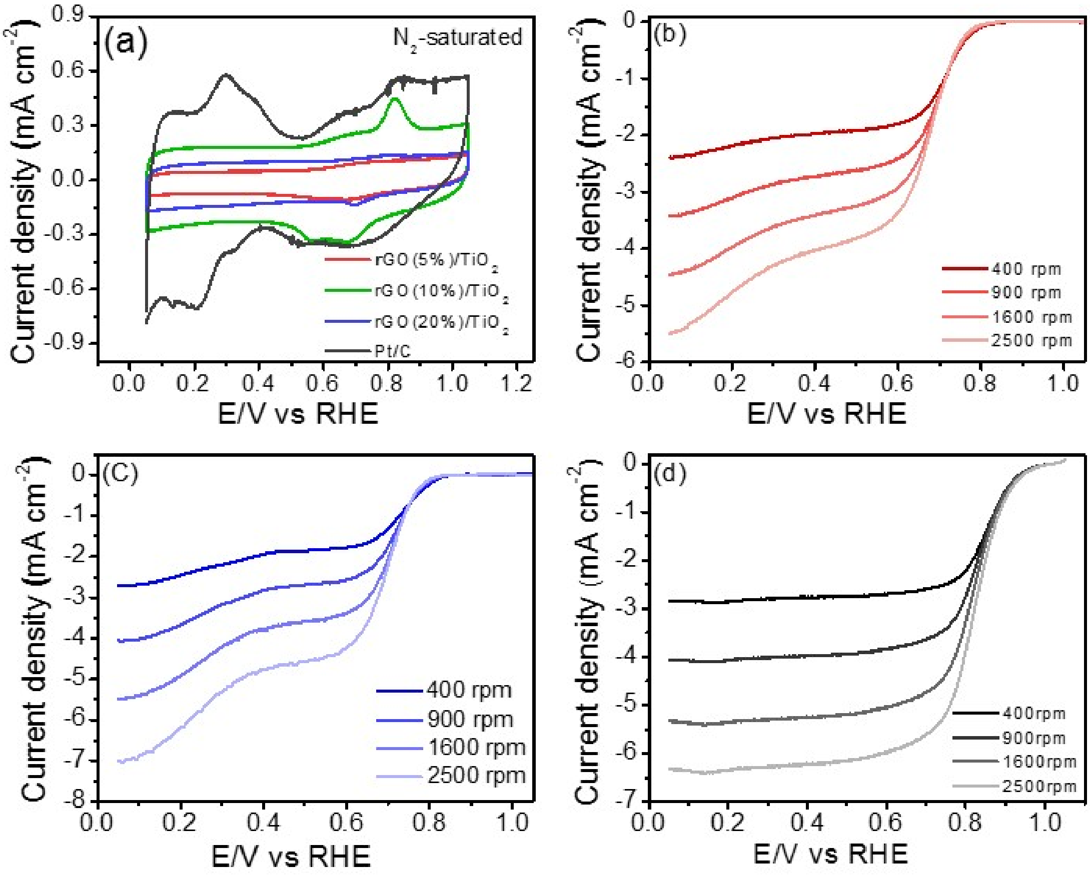

Fig. S8 (a) CV curves of various samples on glassy carbon electrodes in N_2-saturated 0.1M KOH. LSV curves of (b) rGO(5%)/TiO_2 (c) rGO(20%)/TiO_2 and (d) Pt/C in O_2-saturated 0.1M KOH with a sweep rate of $5mVs^{-1}$ at the different rotation rates indicated.

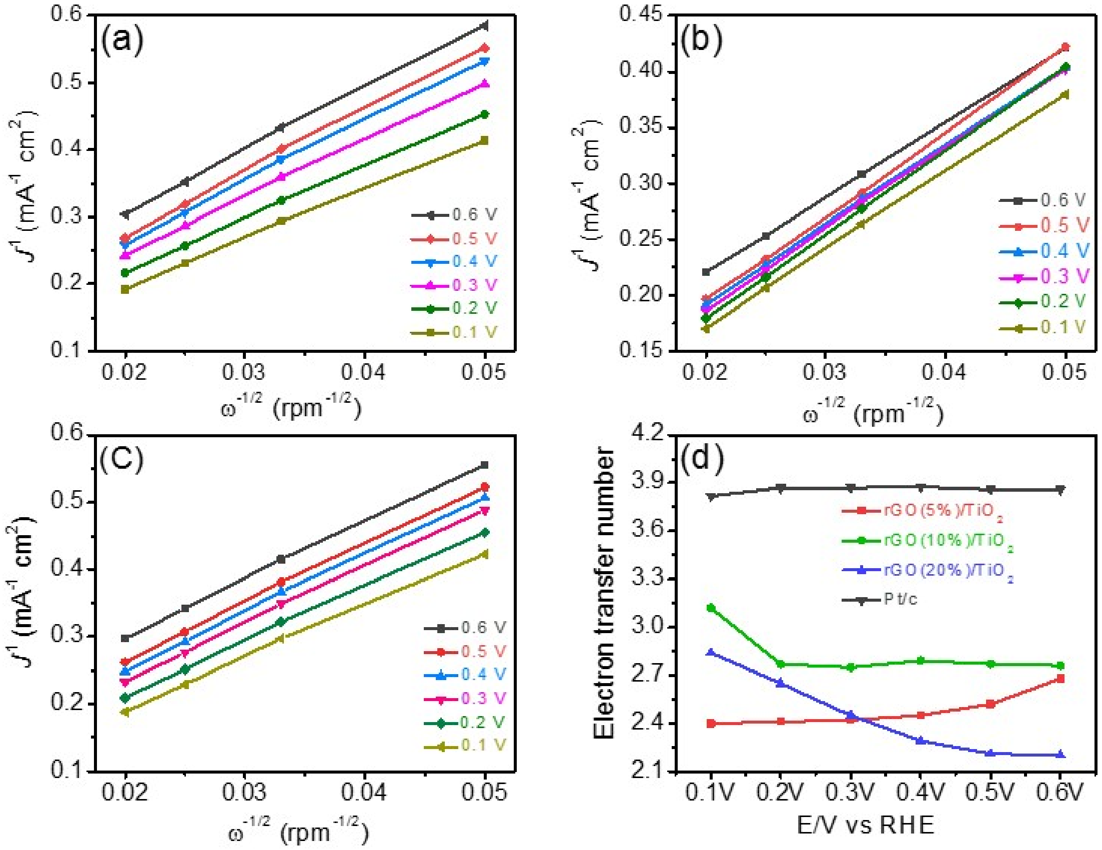

Fig. S9 K-L plots for the (a) rGO(5%)/TiO_2, (b)) rGO(10%)/TiO_2, (c) rGO(20%)/TiO_2 derived from corresponding ORR plots at different potentials and (d) electron transfer number of rGO(5%)/TiO_2, rGO(10%)/TiO_2, rGO(20%)/TiO_2 and Pt/C

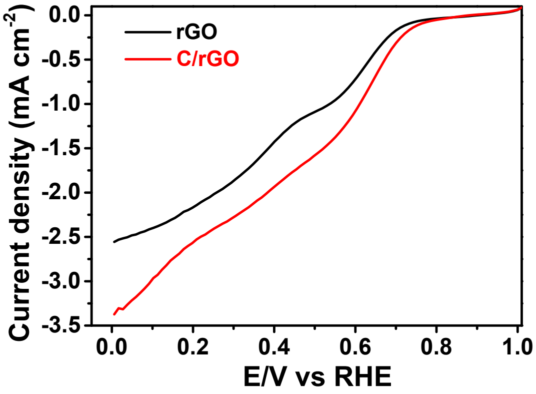

Fig. S10 LSV curves of rGO and C/rGO in O_2-saturated 0.1M KOH with a sweep rate of 5mVs^{-1} at the 1600 rotation rates indicated.

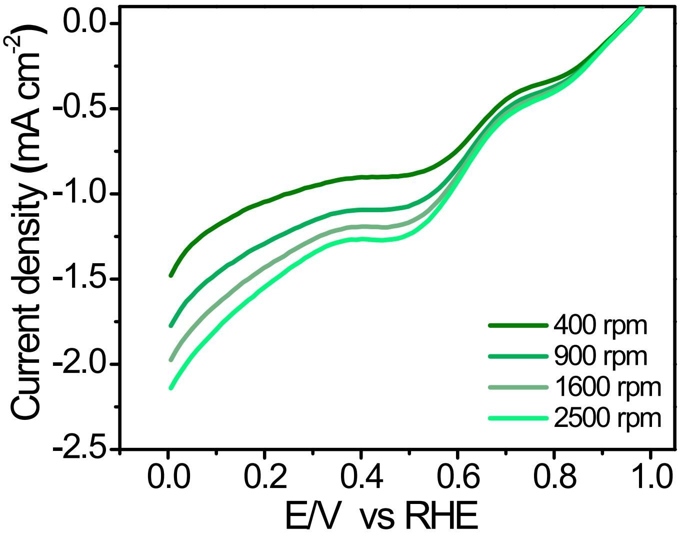

Fig. S11 LSV curves of non-hollow rGO(10%)/TiO_2 in O_2-saturated 0.1M KOH with a sweep rate of 5mVs^{-1} at the different rotation rates indicated.

Table S2. Summary and comparison of ORR activity of our catalysts with the similar composite structures reported in the literature

Serial Number	Sample disruption	Electrolyte	Onset potential	Half-wave potential	References
1	N-Doped TiO_2 Nanorods-Graphene	0.1 M KOH	5 mV (E vs Hg/HgO)	70 mV (E vs Hg/HgO)	[4]
2	N-doped C-embedded TiO_2 nanofibers	0.5 M KOH	-11 mV (E vs Ag/AgCl)	217 mV (E vs Ag/AgCl)	[5]
3	rGO-TiO2	0.1 M KOH	-200 mV E vs Hg/Hg_2Cl_2	-	[6]
4	Defective TiO_2-rGO	0.1 M KOH	-300 mV (E vs SCE)	-600 mV (E vs SCE)	[7]
5	Defective TiO2-supported Cu nanoparticles	0.1 M KOH	740 mV (E vs RHE)	-	[8]
6	Ti^{3+}-self doped and carbon coated TiO2-rGO	1 M KOH	700 mV (E vs RHE)	820 mV (E vs RHE)	This work

References

1 W. S. Hummers and R. E. Offeman, *J. Am. Chem. Soc.*, 1958, **80**, 1339.

2 B. H. Toby and R. B. Von Dreele, *J. Appl. Crystallogr.*, 2013, **46**, 544.

3 Y. Li, W. Zhou, H. Wang, L. Xie, Y. Liang, F. Wei, J.-C. Idrobo, S. J. Pennycook and H. Dai, *Nat. Nanotechnol.*, 2012, **7**, 394.

4 W. Yuan, J. Li, L. Wang, P. Chen, A. Xie and Y. Shen, *ACS Appl. Mater. Interfaces*, 2014, **6**, 21978.

5 D. Hassen, M. A. Shenashen, S. A. El-Safty, M. M. Selim, H. Isago, A. Elmarakbi, A. El-Safty and H. Yamaguchi, *J. Power Sources*, 2016, **330**, 292.

6 J. Yu, Z. Liu, L. Zhai, T. Huang and J. Han, *Int. J. Hydrogen Energy*, 2016, **41**, 3436.

7 D.-N. Pei, L. Gong, A.-Y. Zhang, X. Zhang, J.-J. Chen, Y. Mu and H.-Q. Yu, *Nat. Commun.*, 2015, **6**, 8696.

8 K. Liu, Y. Song and S. Chen, *Nanoscale*, 2015, **7**, 1224.